HTML ABSTRACT + LINKS

APPLIED PHYSICS LETTERS VOLUME 85, NUMBER 18 1 NOVEMBER 2004

Atomic-scale structural analyses of epitaxial Co/Re superlattices

Wentao Xu[a] and Lance E. De Long
Department of Physics and Astronomy, University of Kentucky, Lexington, Kentucky 40506

Timothy Charlton
Materials Science Division, Argonne National Laboratory, Argonne, Illinois 60439

Matthew Chisholm
Oak Ridge National Laboratory, P. O. Box 2008, MS6030-Oak Ridge, Tennessee 37831

David Lederman
Department of Physics, West Virginia University, Morgantown, West Virginia 26506

(Received 28 June 2004; accepted 16 September 2004)

High-resolution transmission electron microscopy and scanning transmission electron microscopy (STEM) have been used to investigate atomic-scale structural properties of Co/Re trilayers and superlattices grown via magnetron sputtering. The sample growth was epitaxial with the $(10\bar{1}0)$ plane of Co and Re parallel to the $(11\bar{2}0)$ plane of Al_2O_3, and the [001] direction of Re and Co coinciding with that of the Al_2O_3. Both low-angle and high-angle *Z*-contrast STEM images show a very uniform layer thickness. However, the interface roughness between the Re and Co layers monotonically increases with interface distance from the substrate. These results strongly imply that, in the epitaxial Re/Co superlattice system, interface roughness plays a more important role in the giant magnetoresistance effect than thickness fluctuations of the spacer layer. Previous anisotropic magnetoresistance measurements can be explained in terms of the observed atomic-scale structure. © *2004 American Institute of Physics*. [DOI: 10.1063/1.1813626]

Giant magnetoresistance (GMR) has been attributed to spin-dependent scattering of conduction electrons, both in the bulk and at the interfaces, in film materials.[1,2] For example, in polycrystalline Fe/Cr superlattices, both a reduction[3] and an increase[1] of the GMR effect with increasing interface roughness have been reported. For Co/Pd superlattices, the first system reported to have perpendicular magnetic anisotropy,[4] the Pd polarization is found to be very sensitive to structural defects.[5] Other studies show that GMR depends on the thickness fluctuation of spacer layers between magnetic films.[6,7] Therefore, an important question is exactly how the GMR effect is related to the structural properties of the superlattices. The ambiguities in the experimental data may be due, at least in part, to the difficulty of quantitatively measuring the local *atomic-scale* structure of superlattices, and especially of their local interface structure.

High-resolution transmission electron microscopy (HRTEM) and scanning transmission electron microscopy (STEM) permit atomic analysis of material structures. *Z*-contrast STEM is particularly useful for characterization of structures composed of different elements. In this letter, HRTEM and *Z*-contrast STEM were combined to analyze Co/Re superlattices that exhibit both GMR and anistropic magnetoresistance (AMR). GMR and AMR can compete or reinforce each other, depending upon the directions of the *c* axis of the superlattice and the applied current with respect to the external magnetic field.[8–10] These properties can be used to determine whether spin-dependent scattering occurs preferentially at the interface or in the bulk of the layers.[9,10] We show that these transport properties are best understood by taking into account the directly measured atomic-scale structure of the superlattice.

Re(5 nm)/Co(30 nm)/Re(2 nm) trilayer and Re(5 nm)/(Co(2 nm)/Re(3 nm))$_{19}$ superlattice samples were grown on $(11\bar{2}0)Al_2O_3$ substrates via dc magnetron sputtering with a base pressure of 3.0×10^{-7} Torr. A 5-nm-thick Re buffer layer was first grown on the substrate at 560 °C. The superlattice and trilayer were then grown at 165 °C to maximize crystallinity and minimize interdiffusion across layers. A dedicated STEM (VG 501 operated at 100 kV) and a HRTEM (JEOL 2010F operated at 200 kV) were used for *Z*-contrast and crystal structure analysis, respectively.

HRTEM analysis of the trilayer sample was performed with the electron beam directed along the *c* direction of the Al_2O_3 substrate. Atomic-resolution images of the trilayer are shown in Fig. 1. The substrate–buffer and buffer–Co interfaces are shown in Fig. 1(a). Figure 1(b) and 1(c) reveal a nearly perfect alignment of the growth orientation of the Co and Re layers. Moreover, Re and Co layers exhibit high-quality epitaxial growth with their $(10\bar{1}0)$ planes parallel to the $(11\bar{2}0)$ planes of the Al_2O_3; and the [001] direction of Re and Co coincides with that of the Al_2O_3. Atomic-resolution images of the top Co–Re and Re–vacuum interfaces of the trilayer sample were also obtained (not shown). The well-defined hexagonal structure confirmed the epitaxial growth of the top Re layer on the Co layer, even though the top Re layer thickness was only ~2.14 nm thick. We noted that some Re atoms were missing or overgrown along the edge of the top surface and formed a zigzag structure. We believe this is the intrinsic structure of the superlattice because a very thin layer of bonding material used in the cross-sectional TEM sample preparation remained in place to pro-

[a]Author to whom correspondence should be addressed; electronic mail: wxu2@uky.edu

 © 2004 American Institute of Physics
Downloaded 07 Dec 2004 to 128.219.12.140. Redistribution subject to AIP license or copyright, see http://apl.aip.org/apl/copyright.jsp

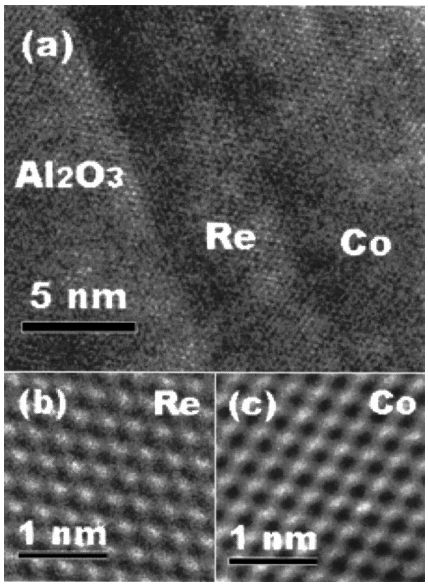

FIG. 1. HRTEM images of: (a) bottom Al_2O_3–Re and Re–Co interfaces, (b) Re atomic structure, and (c) Co atomic structure, of the trilayer sample. Light and dark shading in (a) reflect image contrast generated by thickness variations near the sample surface.

tect the surface. There were no obvious defects observed in the thick Co layer.

Figure 2 shows a *Z*-contrast STEM image of the trilayer sample, and the inset is an overall view of the sample cross section. The layer thickness and interface roughness parameters obtained from the above analyses mentioned are shown in Table I. Note that the Re edge is quite continuous and has very few voids, and clear Re steps can be seen at the Re/Co interface in Fig. 2. The clear and sharp edge indicates that the Re(Co) atoms tend to bind together and form a compact boundary in order to reduce their binding/surface energy. Therefore, the surface/interface roughness in the Co/Re superlattice is dominated by edge steps, implying interdiffusion between Co and Re is very weak (no more than one monolayer on average).

In order to measure the interface roughness, we defined a line that best defined an average boundary between the layers, and measured the distances between the line and the local boundary between Re and Co atoms, then calculated the rms roughness for a large number of locations along the interface. For simplicity, the measured points on a local

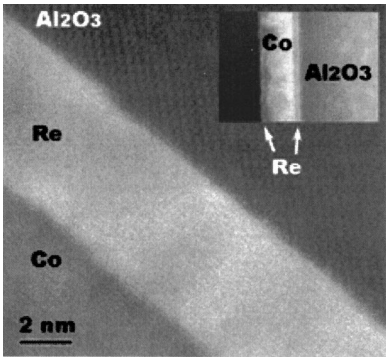

FIG. 2. High-angle annular dark-field (*Z*-contrast) STEM image of the bottom Al_2O_3–Re and Re–Co interfaces. The inset is a low-magnification view of the trilayer sample cross section that shows the two thinner Re layers bounding the thicker Co layer.

TABLE I. Parameters from HRTEM and STEM analysis. t and σ represent the layer thickness and rms interface roughness. $\sigma_{\text{sub-buf}}$, $\sigma_{\text{buf-Co}}$, $\sigma_{\text{Co-Re}}$, and $\sigma_{\text{Re-air}}$ denote the interface roughness between Al_2O_3 substrate and Re buffer, Re buffer and bottom Co, bottom Co and Re, and top Re and air, respectively. Units are nanometers.

	t_{Re}	t_{Co}	t_{buf}	$\sigma_{\text{sub-buf}}$	$\sigma_{\text{buf-Co}}$	$\sigma_{\text{Co-Re}}$	$\sigma_{\text{Re-air}}$
Trilayer	2.14	29.50	5.06	0.12	0.21	0.93	1.30
Superlattice	2.95	2.07	5.08	0.10	0.17	0.21	0.72

boundary were chosen representatively rather than randomly; and the low atomic interdiffusion permitted us to estimate their distribution probabilities as weighting factors in the calculation of the rms roughness. The roughness values are consistent with, but a little bit smaller than, the previous x-ray reflectivity (XRR) measurements of other Co/Re superlattices.[8,9] If the weak interdiffusion is included, the interface roughness values are in good agreement with that measured by XRR[8,9] since XRR cannot distinguish between step disorder and interdiffusion.

HRTEM images of the superlattice were observed with the electron beam oriented along the $[\bar{1}10]$ direction of the Al_2O_3 substrate, as shown in Fig. 3. The two-dimensional lattice structures in Fig. 3(a) exhibit a high-quality epitaxial growth of the buffer layer over the Al_2O_3 substrate. More

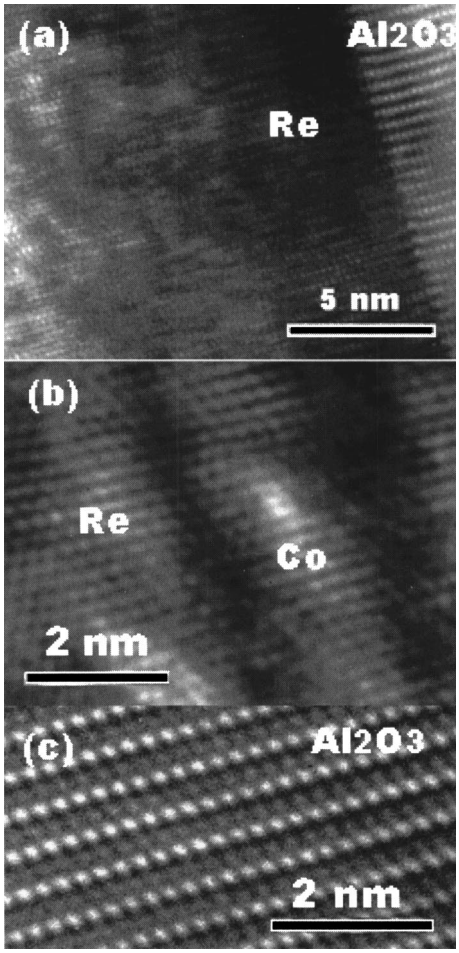

FIG. 3. HRTEM images of: (a) bottom part of the superlattice, (b) atomic structure of Re and Co layers, and (c) atomic structure of Al_2O_3 for the superlattice sample. Light and dark patches in (a) and (b) are due to thickness variations near the sample surface.

Downloaded 07 Dec 2004 to 128.219.12.140. Redistribution subject to AIP license or copyright, see http://apl.aip.org/apl/copyright.jsp

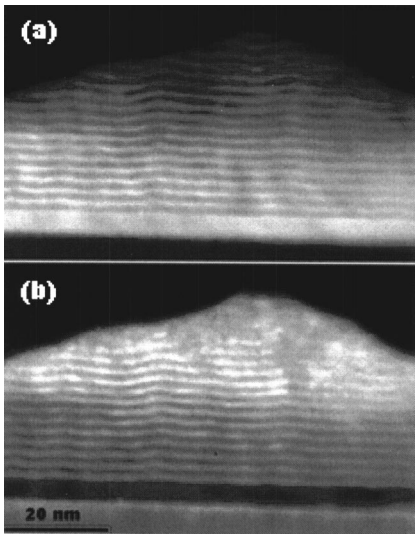

FIG. 4. (a) High-angle annular dark field (*Z*-contrast) and (b) low-angle annular dark-field STEM images of the Co/Re superlattice sample. The white and dark bands correspond to Re, Co in (a) and Co, Re in (b), respectively.

details of the crystal structure are clearly shown in Figs. 3(b) and 3(c). A Re buffer layer of ~5.10 nm thickness permits the Co/Re superlattice to grow expitaxially over the $(11\bar{2}0)$ plane of the substrate. The $(\bar{2}110)$ plane of both Re and Co are parallel to the $(\bar{1}100)$ plane of the Al_2O_3, which means that Re and Co grow with their $(10\bar{1}0)$ planes parallel to the $(11\bar{2}0)$ planes of Al_2O_3, and that the [001] direction of Re and Co coincides with that of the Al_2O_3. This epitaxial relationship is identical to that observed for the trilayer sample. Detailed analyses indicate that the two-dimensional lattice spacings for Co, Re, and Al_2O_3 are approximately 0.24 and 0.43 nm, 0.26 and 0.44 nm, and 0.24 and 0.44 nm, respectively. These lattice spacings closely correspond to $a/2$ and $c/3$, where a and c are lattice parameters of bulk Al_2O_3. There were no obvious defects observed within Re and Co layers, but a few voids were found at interface locations.

STEM observations of the superlattice with the electron beam directed along the $[\bar{1}10]$ direction of the Al_2O_3 substrate are shown in Fig. 4. Both high-angle annular dark field (*Z* contrast) and low-angle annular dark field STEM images [see Figs. 4(a) and 4(b), respectively], exhibit a very uniform period thickness, independent of the image contrast. Layer thickness and interface roughness were measured with the help of higher magnification analysis and are listed in Table I. Although the surface/interface roughness values are quite small, they correlate with the amount of substrate surface roughness, and a clear evolution of the surface/interface roughness can be seen: Starting from the substrate surface, the interface roughness is correlated from interface to interface, and amplified with increasing distance of the interface from the substrate. A similar correlated roughness behavior has been observed in Nb/Si multilayers grown via sputtering at higher Ar pressures.[11] Compared to the interface layer thickness or interface roughness, the layer thickness fluctuations are relatively small.

GMR depends only on the relative orientation of the magnetic moments of the layers, whereas AMR depends on the anisotropic electron scattering caused by the spin–orbit interaction.[12,13] Therefore, the GMR and AMR resistivities can be independently added to form the total MR in Co/Re superlattice. The epitaxial growth of the Co and Re layers with their $(10\bar{1}0)$ planes parallel to the $(11\bar{2}0)$ of the Al_2O_3 substrate and with the *c*-axis in-plane, makes the superlattice anisotropic, with the magnetic easy axis along the $\boldsymbol{c}$ direction. Because of this, the GMR is different in the $\mathbf{I}\|\boldsymbol{c}$ and $\mathbf{I}\perp\boldsymbol{c}$ configurations, where $\mathbf{I}$ is the applied current.[9] Because the AMR is much larger when $\mathbf{I}\|\boldsymbol{c}$ than when $\mathbf{I}\perp\boldsymbol{c}$,[9] and is dominated by bulk scattering, spin-dependent interface scattering is expected to play a more significant role in MR when $\mathbf{I}\perp\boldsymbol{c}$ than when $\mathbf{I}\|\boldsymbol{c}$. *This is exactly what was found in previous experiments*.[8,9] Since the crystalline defects were mainly observed at interface locations rather than within the Co layers, the spin-dependent scattering of conduction electrons mainly occurs at the interface regions. Considering that GMR depends on the amount of spin-dependent scatterings of conduction electrons inside each ferromagnetic layer or at the interfaces, we infer that in Co/Re superlattices the GMR spin-dependent scattering occurs mainly at the interfaces, i.e., *interface roughness plays a dominant role in the observed GMR*. This is in agreement with what was indirectly inferred from the temperature dependence of the GMR of the Co/Re superlattices.[9]

In conclusion, we have directly imaged the atomic-scale structure of Co/Re trilayers and superlattices using HRTEM and *Z*-contrast STEM. Co and Re grow epitaxially with the $(10\bar{1}0)$ plane parallel to the $(11\bar{2}0)$ plane of Al_2O_3, and the [001] direction of Re and Co coincides with that of the Al_2O_3. Layer thickness fluctuations are relatively small compared to interface roughness, implying that interface roughness plays a dominant role in the observed GMR of the epitaxial Re/Co superlattice system. Existing anisotropic MR data[8,9] are fully consistent with these directly observed structural properties.

This work was supported by The University of Kentucky Office of Graduate Studies and Research and by NSF-EPSCoR Grant No. EPS-0083046 at both the University of Kentucky and West Virginia University. The research at Oak Ridge National Laboratory was supported by the U.S. Department of Energy under Contract No. DE-AC05-00OR22725.

[1] E. E. Fullerton, D. M. Kelly, J. Guimpel, and I. K. Schuller, Phys. Rev. Lett. **68**, 859 (1992).
[2] M. Suzuki and Y. Taga, Phys. Rev. B **52**, 361 (1995).
[3] R. Schad, P. Beliën, G. Verbanck, C. D. Potter, H. Fisher, S. Lefebvre, M. Bessiere, V. V. Moshchalkov, and Y. Bruynseraede, Phys. Rev. B **57**, 13692 (1998).
[4] P. F. Carcia, A. D. Meinhaldt, and A. Sunna, Appl. Phys. Lett. **47**, 178 (1985).
[5] J. R. Childress, R. Kergoat, O. Durand, J.-M. George, P. Galtier, J. Miltat, and A. Schuhl, J. Magn. Magn. Mater. **130**, 13 (1994).
[6] S. S. Parkin, Phys. Rev. Lett. **71**, 1641 (1993).
[7] B. Dieny, J. Magn. Magn. Mater. **136**, 335 (1994).
[8] T. Charlton, D. Lederman, S. M. Yusuf, and G. P. Felcher, J. Appl. Phys. **85**, 4436 (1999); T. Charlton, J. McChesney, D. Lederman, F. Zhang, J. Z. Hilt, and M. J. Pechan, Phys. Rev. B **59**, 11897 (1999).
[9] T. Charlton and D. Lederman, Phys. Rev. B **63**, 094404 (2001).
[10] W. Burgei, M. J. Pechan, T. Charlton, and D. Lederman, J. Appl. Phys. **91**, 7529 (2002).
[11] E. E. Fullerton, J. Pearson, C. H. Sowers, S. D. Bader, X. Z. Wu, and S. K. Sinha, Phys. Rev. B **48**, 17432 (1993).
[12] H. J. F. Jansen, Phys. Today **48**, 50 (1995).
[13] G. A. Prinz, Phys. Today **48**, 58 (1995).

Downloaded 07 Dec 2004 to 128.219.12.140. Redistribution subject to AIP license or copyright, see http://apl.aip.org/apl/copyright.jsp